SIMPLIFIED NONQUASI-STATIC FET MODELLING APPROACH EXPERIMENTALLY VALIDATED UP TO 118.5 GHZ

M. Fernández-Barciela, P. J. Tasker*, M. Demmler‡,Y. Campos-Roca, H. Massler‡, E. Sánchez, C. Currás-Francos and M. Schlechtweg ‡

Universidade de Vigo, Spain *University of Wales Cardiff, U.K. ‡Fraunhofer Institute IAF, Freiburg, Germany

ABSTRACT

In this paper two similar simplified nonquasi-static approaches are applied for high-frequency large-signal FET prediction. Both account for low-frequency dispersion and use a simplified extraction process through the use of linear delays. Excellent results are obtained from dc up to the device f_T frequencies, even when f_T is 120 GHz. For low-frequency prediction a simple quasi-static extrinsic approach can produce excellent results thus further simplifying modelling. The influence of including the low-frequency dispersion modelling is also taken into account.

INTRODUCTION

As a general purpose modelling tool (device and process independent, dc and small-large rf signal predictors), table-based empirical models have been successfully used in CAD of MMICs. The dense set of measurements required for an accurate model behaviour and the non-uniqueness of the extracted large-signal relations are some of the disadvantages that have been previously discussed.

It is also important to consider the usable bandwidth of these models. Model improvement at low-frequency can be achieved by accounting for low-frequency dispersion using the Root proposal [1], but that model, as initially published, has important limitations in the high-frequency regime. In general, table-based models have difficulties in including "r_i" type elements (or quadratic frequency dependencies of the y-parameters) in a fully consistent manner. Nonquasi-static approaches have been suggested which model such effects [2,3] through the use of nonlinear delay functions. However, in most cases, the increase in model bandwidth is achieved at the expense of the need for more measurements along with more complex model generation and implementation. Taking those models as starting point, a new modelling approach is suggested, which maintains a wide bandwidth but also has a simplified extraction and implementation approach.

MODELLING APPROACH

The first model (model1) accounts for both the low-frequency dispersion, using a nonquasi-static current formulation, see Root et al.[1], in the input and in the output of the device, and the high-frequency dynamic behaviour, through a nonquasi-static charge formulation, see Daniels et al.[2]. Hence, the current at i-th terminal is (following Root formulation):

$$I_i(t) = h(t)^{-1} I_i^{low}(V_{GS}, V_{DS}) + h(t)^{-1}\tau_x \frac{d}{dt} I_i^{high}(V_{GS}, V_{DS}) + \frac{dQ_i^{nq}(t)}{dt}, \quad h(t) = 1 + \tau_x \frac{d}{dt} \qquad (1)$$

where Q_i^{nq} is in this case the nonquasi-static charge at i-th terminal, expressed as [2]:

$$Q_i^{nq}(t) = Q_i^q(V_{GS}, V_{DS}) - \tau_i(V_{GS}, V_{DS}) \frac{dQ_i^{nq}(V_{GS}, V_{DS})}{dt} \qquad (2)$$

Q_i^q (charge relation) and τ_i (delay relation) are quasi-static functions of nodal voltages. τ_i represents a time for redistribution of charge at i-th terminal. For this model the resulting small-signal y-parameters are [4]:

$$Y_{ik} = i_i / v_k = g_{ik}^{dc} + \frac{j\omega\tau_x}{1 + j\omega\tau_x}(g_{ik}^{ac} - g_{ik}^{dc}) + \frac{j\omega c_{ik}}{1 + j\omega\tau_i} \qquad (3)$$

where $g_{ik}^{dc} = \partial I_i^{low} / \partial V_K$, $g_{ik}^{ac} = \partial I_i^{high} / \partial V_K$, $c_{ik} = \partial Q_i^q / \partial V_K$, i=G,D, $V_K = V_{GS}, V_{DS}$ and $v_k = v_{gs}, v_{ds}$. Model2 is formulated by considering an approximation of eq. 2, suggested in [4,5].

$$Q_i^{nq}(t) \approx Q_i^q(V_{GS},V_{DS}) - \tau_i(V_{GS},V_{DS})\frac{dQ_i^q(V_{GS},V_{DS})}{dt} \quad (4)$$

In this case the following small-signal y-parameters result:

$$Y_{ik} = g_{ik}^{dc} + \frac{j\omega\tau_x}{1+j\omega\tau_x}(g_{ik}^{ac} - g_{ik}^{dc}) + j\omega(1-j\omega\tau_i)c_{ik} \quad (5)$$

Equations 3 and 5 can be analyzed in three different cases:

a) $\omega \to 0$. DC case. In both approaches

$$Y_{ik} \approx g_{ik}^{dc} \quad (6)$$

b) $\omega\tau_x >> 1$.

$$Y_{ik} \approx g_{ik}^{ac} + \frac{j\omega c_{ik}}{1+j\omega\tau_i} \qquad \text{model1} \quad (7)$$

$$Y_{ik} \approx g_{ik}^{ac} + \omega^2\tau_i c_{ik} + j\omega c_{ik} \qquad \text{model2} \quad (8)$$

c) $\omega\tau_x >> 1$ and $\omega\tau_i << 1$. In both models

$$Y_{ik} \approx g_{ik}^{ac} + j\omega c_{ik} \quad (9)$$

as can be obtained in Root model in the range when $\omega\tau_x >> 1$. Eq. 8 is a frequency approximation of model1 when $\omega^2\tau_i^2 << 1$. It is not as restrictive as Root approach and is able to model the high-frequency quadratic dependencies of the y-parameters given in model2. As it will be demonstrated, both models can predict excellent results at least up to f_T.

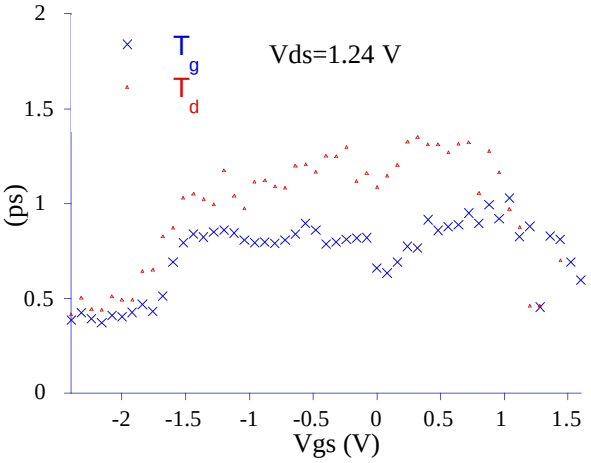

Figure 1: Input and output delay functions vs. gate voltage. 0.6x100 μm^2 P-HEMT. Frequency range for extraction 0.5 to 40 GHz.

g_{ik}^{ac}, c_{ik} and τ_i are determined from the small-signal y-parameters measured in the frequency range where $\omega\tau_x >> 1$(i.e. using eq. 7 in model1 and eq. 8 in model2). This 'curve-fitting' has been performed using robust estimation in order to minimize the contributions of noisy data to the generation process [4]. Once these parameters are obtained versus bias, it is possible to generate I_i^{high} and Q_i^c through a theoretically path-independent contour integral process. I_i^{low} relations are obtained from DC measurements.

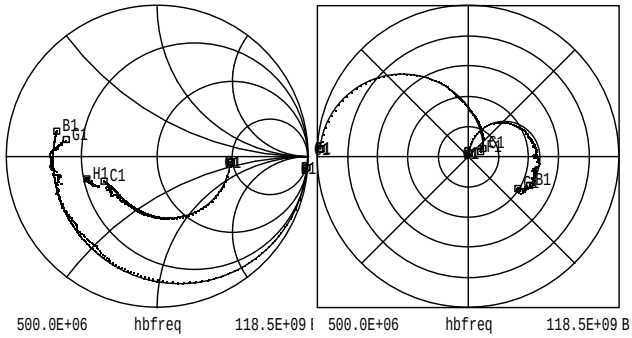

Figure 2: Measured (doted) and simulated (line) s-parameters. 0.15x120 μm^2 P-HEMT. Frequency range: 0.5 to 118.5 GHz. Vgs0=0.3 V, Vds0=1.5 V.

When generating these models, it is necessary to perform multifrequency s-parameter measurements in a fine mesh of bias; this is a very time consuming process. To overcome that a constant τ_i function was used (as suggested in [5]) which allows for simplified model extraction, generation and implementation. Figure 1 shows an example of the bias dependence of the delay function in the input and output of the device for model1. It can be seen that τ_i is a weak function of bias in most of the I-V range. By considering it a constant, it is possible to extract g_{ik}^{ac} and c_{ik} from single frequency measurements using eq. 9 in both models (as in Root approach). Afterwards, it is only necessary to perform a reduced set of measurements over frequency at various bias points to extract, using eq. 7 for model1 or 8 for model2, an estimation of the constant value for τ_i.

DISCUSSION

Models 1 and 2 have been generated for 120 GHz f_T P-HEMT δ-doped devices fabricated at the

Fraunhofer Institut (IAF). S-parameters measurements from 0.5 to 120 GHz have been performed using the system described in [6] and they have been used for parasitic extraction and model validation. For nonlinear model extraction, we have used dc and s-parameters Bias Scans, as proposed in [7], allowing a quick way of obtaining a detailed nonlinear device characterization. The measured bias dependent 2 GHz intrinsic s-parameters were used to generate the intrinsic large-signal constitutive relations [5].

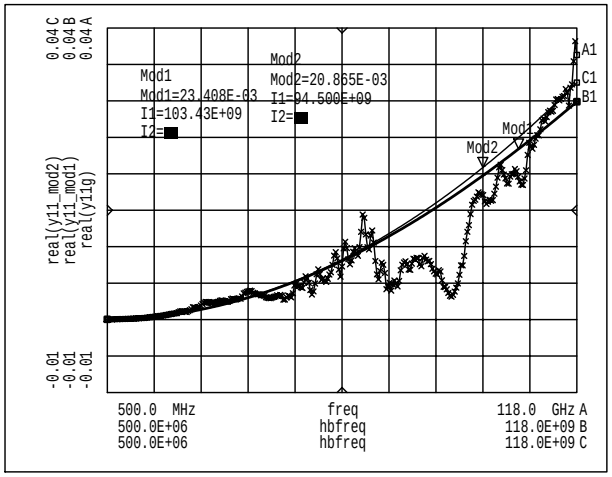

Figure 3: Measured (star) and simulated (line) intrinsic y_{11} parameter. 0.15x120 μm^2 P-HEMT. Frequency range : 0.5 to 118.5 GHz. Bias: Vgs0=0.3 V, Vds0=1.5 V.

For extracting τ_i values, measurements were performed in the range 0.5 to 50 GHz (for both models) in various bias points. A rough estimation of τ_i can also be obtained from classical linear models; for example, τ_g can be obtained from $r_i * c_{gs}$ product. Large-signal measurements have been done using an on-wafer vector-calibrated large-signal measurement system [8]. Both models were implemented in MDS and simulated under dc, small and large-signal excitations. Figure 2 shows a comparison between measured and simulated using model 2 s-parameters in the range 0.5 GHz to 118.5 GHz. Excellent agreement can be observed up to 118.5 GHz. Assuming the use of the same delay in both models, figure 3 shows the intrinsic y_{11} vs. frequency measured and simulated using models 1 and 2. Very little difference can be observed even at very high frequencies, confirming that model2 is a very good approximation of model1. Figure 4 compares measured and simulated output power levels versus input power for the fundamental (16 GHz) and second harmonic using model2. Similar excellent results have been obtained in the range of fundamental frequencies checked from 2 to 20 GHz. Figure 5 compares measured and simulated large-signal dynamic loadline at a fundamental frequency of 20 GHz. Not only the rf global behaviour can be predicted using both models but also the rf dynamic behaviour and the static dc bias point. The last is possible due to the inclusion of the low-frequency dispersion in the model formulation (as discussed later). In the case of working in the low-frequency range, even if these models can accurately predict device behaviour, we can further simplify model formulation. Figure 6 shows the good agreement obtained using an extrinsic model based on eq. 1 but considering only pure quasi-static charge nonlinear relations (as in [1]). If we also drop in this extrinsic approach the low-frequency dispersion modelling, using a single current generator in each port, there is a loss in the accuracy of the dc current prediction, as can be seen in figure 7.

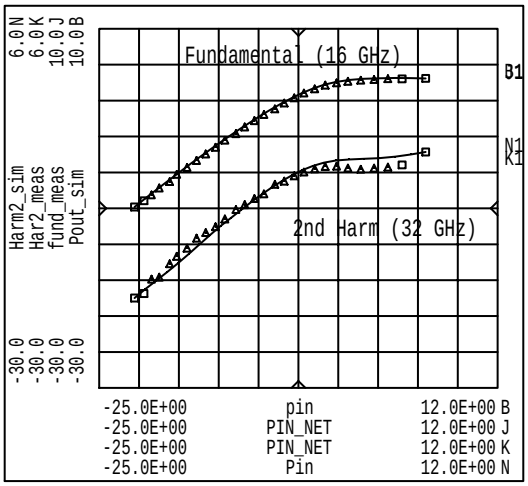

Figure 4: Measured (triangles) and simulated (line) fundamental (dBm) and second harmonic(dBc) power levels. 0.15x120 μm^2 P-HEMT. Fundamental freq.: 16 GHz. Bias: Vgs0=0.3 V, Vds0=0.5 V.

CONCLUSIONS

Two similar nonquasi-static modelling approaches have been implemented and discussed. In both, model extraction and implementation are extremely simple. They can be extracted from dc and small-signal s-parameters. Excellent results have been obtained with P-HEMT devices under small and large-signal excitation. Both can be

successfully used from dc up to at least the f_T frequency of the device.

REFERENCES

[1] D. E. Root, S. Fan, J. Meyer, "Technology Independent Large-Signal FETs Models: A Measurement-Based Approach to Active Device Modelling," 1991, Proc. 15th ARMMS Conference.

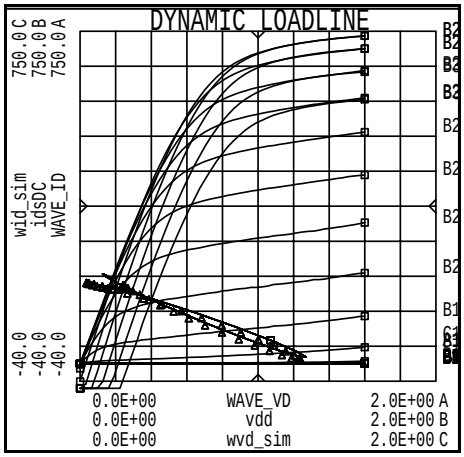

Figure 5: Measured (triangles) and simulated (line) dynamic loadline (on the back, the dc simulated I-V curves). 0.15x120 μm^2 P-HEMT. Fundamental freq.: 20 GHz. Bias point: Vgs0=0.3 V, Vds0=0.5 V.

[2] R. R. Daniels, J. P. Harrang, A. Yang, " A Nonquasi Static, Large-signal FET Model Derived from Small-signal S-parameters," 1991, Proc. International Semiconductor Device Research Symposium, p. 601.

[3] M. C. Foisy, P. E. Jeroma, G. H. Martin, "Large-Signal Relaxation-Time Model for HEMTs and MESFETs," 1992, IEEE MTT-S, pp. 251-254.

[4] M. Fernández Barciela "Contribución al modelado no lineal del MODFET basado en tablas," 1996, Ph.D. Dissertation.

[5] M. Fernández Barciela, P.J. Tasker, M. Demmler, E. Sánchez, "A simplified nonquasi-static table-based FET Model," 1996, 26th EuMC, pp. 20-23.

[6] P.J. Tasker and J. Braunstein. "A New MODFET Small-signal Circuit Model required for Millimeter-Wave MMIC Design: Extraction and Validation to 120 GHz", Proc. 1995 IEEE MTT-S, pp. 611-615.

[7] M. Fernández Barciela, P.J. Tasker, M. Demmler, J. Braunstein, B. Hughes, E. Sánchez, "Novel Interactive Measurement and Analysis System for Large-signal Characterization of FETs," 1994, 18th European Workshop on Compound Semiconductor Devices and Integrated Circuits, pp.16-17.

[8] M. Demmler, P. J. Tasker, M. Schlechtweg. " A Vector Corrected High Power On-Wafer Measurement System with a frequency Range for the higher Harmonics up to 40 GHz," 1994, Proc. 24th EuMC, pp. 1367-1372 .

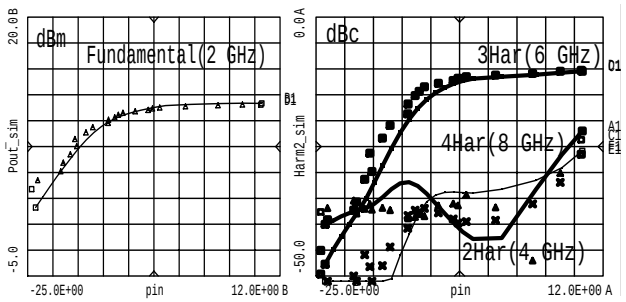

Figure 6: Measured (triangles) and simulated (line) output power levels vs. input power. 100x0.6 μm^2 P-HEMT device. Model extraction: 2GHz. Fundamental freq.: 2GHz.

ACKNOWLEDGMENTS

The authors would like to thank the Fraunhofer Institut and D. E. Root for their co-operation. This work was partly supported by the Spanish Ministerio de Educación y Ciencia and the regional government Xunta de Galicia.

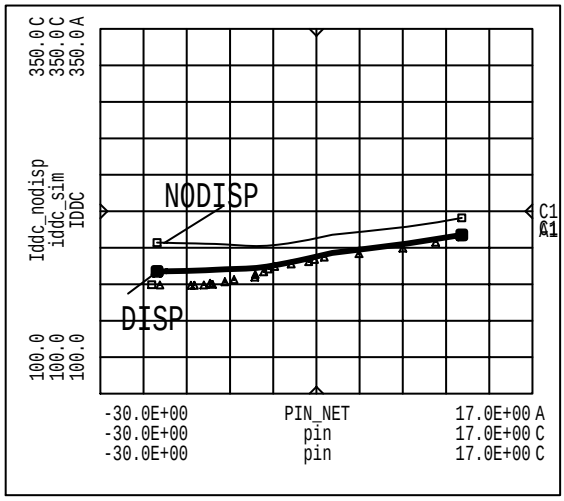

Figure 7: Output dc current (mA/mm) vs. input power measured (triangles) and simulated using an extrinsic approach with (thick line) and without (thin line) the low-frequency dispersion modelling. 100x0.6 μm^2 P-HEMT device. Model extraction: 2GHz. Fundamental freq.: 2GHz.